Solving elliptic eigenvalue problems on polygonal meshes using discontinuous Galerkin composite finite element methods

Stefano Giani

School of Engineering and Computing Sciences, Durham University , South Road, Durham, DH1 3LE United Kingdom

Abstract

In this paper we introduce a discontinuous Galerkin method on polygonal meshes. This method arises from the Discontinuous Galerkin Composite Finite Element Method (DGFEM) for source problems on domains with micro-structures. In the context of the present paper, the flexibility of DGFEM is applied to handle polygonal meshes. We prove the a priori convergence of the method for both eigenvalues and eigenfunctions for elliptic eigenvalue problems. Numerical experiments highlighting the performance of the proposed methods for problems with discontinuous coefficients and on convex and non-convex polygonal meshes are presented.

1 Introduction

In recent years people have realised the gain in flexibility coming from polygonal and polyhedral meshes, for this reason many finite element methods have been developed to accommodate such meshes. In the continuous Galerkin setting we have the composite finite element methods (CFEs) [1, 2, 3, 4, 5], the polygonal finite element methods (PFEMs) [6, 7], the extended finite element method (XFEM) [8] and the virtual finite element method (VFEM) [9]. On the other hand in the discontinuous Galerkin (DG) setting we have the interior penalty methods on polygonal and polyhedral meshes [10], the

agglomeration-based method [11, 12, 13] and the discontinuous Galerkin composite finite element methods (DGCFEMs) [14].

One clear advantage in using general polygonal/polyhedral elements is the possibility to mesh complicated shapes and even small geometrical details in the domain. In this direction both the both continuous Galerkin CFE method [1, 2, 3, 4, 5] and discontinuous Galerkin CFE method [15, 14, 16] are capable to solve problems on domains with micro-structures. It is interesting to notice that on domains without small features or micro-structures, DGCFEM [14] and the interior penalty methods on polygonal and polyhedral meshes [10] are closely related. Form an a priori convergence point of view, the main difference between these two methods is the way in which degeneration of edges or faces in the mesh is treated in the theory.

In this work we would like to study the use of polygonal/polyhedral meshes for eigenvalue problems. In our opinion, this seems the natural next step since so many methods for linear/non-linear source problems are already available for such meshes. Comparing the extensions of continuous and discontinuous Galerkin methods to general polygonal/polyhedral meshes, clearly in the DG setting the extension is simpler. For this reason we adopted DG as our starting point. Among all the available DG methods, we choose to apply DGCFEM to eigenvalue problems since $hp-$adaptive scheme are already available for this method [16, 15] and it should be possible in a further work to apply such technologies to eigenvalue problems on general polygonal/polyhedral meshes as well. Moreover, since DGCFEM has been developed to address problems on domains with micro-structures, also the present analysis can be applied to eigenvalue problems on domain with micro-structures using polygonal/polyhedral meshes.

In order to keep the analysis simple, we consider the following model problem: find the eigenpairs (λ, u) such that

$$\begin{cases} -\Delta u &= \lambda\, u \qquad \text{in } \Omega, \\ \\ u &= 0 \qquad \text{on } \partial\Omega. \end{cases} \tag{1}$$

Here, Ω is a bounded, connected polygonal domain in $\mathbb{R}^2$, with boundary $\partial\Omega$. In the rest of the paper we are going to assume that the meshes are constituted by polygonal elements

The outline of the paper is as follows. In Section 2 we describe how the finite element space on polygonal meshes is constructed. In Section 3 we

introduce the discrete version of problem (1) and the discontinuous Galerkin method. In the following Section 4 the a priori analysis is presented and in Section 5 the numerical results are presented. Finally in Section 6 some concluding remarks are collected.

2 Construction of the composite finite element spaces on polygonal meshes

In this section, we describe the construction of the CFE space on a polygonal mesh. The method is inspired by [14], where a similar construction for complicated domain with small features is presented.

The construction of the CFE space takes advantage of two meshes: the polygonal mesh $\mathcal{T}_{\texttt{CFE}}$ and the mesh $\mathcal{T}_h$ constructed splitting the polygons in $\mathcal{T}_{\texttt{CFE}}$ into triangles. By construction the mesh $\mathcal{T}_h$ is finer than the mesh $\mathcal{T}_{\texttt{CFE}}$, in the sense that each element of $\mathcal{T}_h$ has a unique father element in $\mathcal{T}_{\texttt{CFE}}$ such that the father element contains the children element.

2.1 Finite element spaces

We start defining the discontinuous Galerkin finite element space on the mesh $\mathcal{T}_h$, assuming that the polynomial degree is uniformly distributed over the mesh:

$$V(\mathcal{T}_h, p) = \{u \in L_2(\Omega) : u|_\kappa \in \mathcal{P}_p(\kappa),\ \forall \kappa \in \mathcal{T}_h\},$$

where $\mathcal{P}_p(\kappa)$ denotes the set of polynomials of degree at most $p \geq 1$ defined over the general polygon κ. The extension to variable polynomial degrees follows in a natural fashion.

In order to be able to construct the finite element space on the polygonal mesh, we have to assume that the polynomial degree p of the polygonal elements in $\mathcal{T}_{\texttt{CFE}}$ is the same as the polynomial degree of the elements of $\mathcal{T}_h$. In the case of variable polynomial degrees, it is necessary to assume that the polynomial degree of each polygonal element is the same as the polynomial degree of all the children elements.

For each polygonal element $\kappa \in \mathcal{T}_{\texttt{CFE}}$ we define $\hat{\kappa}$ as the smallest rectangle containing κ with edges parallel to the axes. Then the polynomial space $\mathcal{P}_p(\kappa)$ is defined to contain the restriction of the polynomial functions in $\mathcal{P}_p(\hat{\kappa})$ to the support of the element κ. So, the DG finite element space on

the mesh $\mathcal{T}_{\texttt{CFE}}$ is constructed gluing together the polynomial spaces $\mathcal{P}_p(\kappa)$ for all elements $\kappa \in \mathcal{T}_{\texttt{CFE}}$, i.e.;

$$V(\mathcal{T}_{\texttt{CFE}}, p) = \{u \in L_2(\Omega) : u|_\kappa \in \mathcal{P}_p(\kappa),\ \forall \kappa \in \mathcal{T}_{\texttt{CFE}}\}.$$

In view of the definition of $V(\mathcal{T}_{\texttt{CFE}}, p)$, it is clear that the DG space $V(\mathcal{T}_h, p)$ on the finer mesh simplify the construction of the finite element functions on polygons. Any polynomial function in $\mathcal{P}_p(\kappa)$ for any elements $\kappa \in \mathcal{T}_{\texttt{CFE}}$ can be defined as a linear combination of the basis functions living on the children of κ, see [14, Section 8]. So, any integral on polygonal elements or on edges of polygonal elements can be computed as an integral on either elements or edges of the mesh $\mathcal{T}_h$. This is how the method assembles the discrete problem on polygonal meshes.

3 Composite discontinuous Galerkin finite element method

In this section, we introduce the *hp*-version of the (symmetric) interior penalty DGCFEM for the numerical approximation of (1). To this end, we first introduce the following notation.

We denote by $\mathcal{F}^{\mathcal{I}}_{\texttt{CFE}}$ the set of all interior edges of the partition $\mathcal{T}_{\texttt{CFE}}$ of Ω, and by $\mathcal{F}^{\mathcal{B}}_{\texttt{CFE}}$ the set of all boundary edges of $\mathcal{T}_{\texttt{CFE}}$. Furthermore, we define $\mathcal{F} = \mathcal{F}^{\mathcal{I}}_{\texttt{CFE}} \cup \mathcal{F}^{\mathcal{B}}_{\texttt{CFE}}$. The boundary $\partial\kappa$ of an element κ and the sets $\partial\kappa \setminus \partial\Omega$ and $\partial\kappa \cap \partial\Omega$ will be identified in a natural way with the corresponding subsets of $\mathcal{F}$. Let κ^+ and κ^- be two adjacent elements of $\mathcal{T}_{\texttt{CFE}}$, and $\mathbf{x}$ an arbitrary point on the interior edge $F \in \mathcal{F}^{\mathcal{I}}_{\texttt{CFE}}$ given by $F = \partial\kappa^+ \cap \partial\kappa^-$. Furthermore, let v and $\mathbf{q}$ be scalar- and vector-valued functions, respectively, that are smooth inside each element $\kappa^\pm$. By $(v^\pm, \mathbf{q}^\pm)$, we denote the traces of $(v, \mathbf{q})$ on F taken from within the interior of $\kappa^\pm$, respectively. Then, the averages of v and $\mathbf{q}$ at $\mathbf{x} \in F$ are given by

$$\{\!\{v\}\!\} = \frac{1}{2}(v^+ + v^-), \qquad \{\!\{\mathbf{q}\}\!\} = \frac{1}{2}(\mathbf{q}^+ + \mathbf{q}^-),$$

respectively. Similarly, the jumps of v and $\mathbf{q}$ at $\mathbf{x} \in F$ are given by

$$[\![v]\!] = v^+\, \mathbf{n}_{\kappa^+} + v^-\, \mathbf{n}_{\kappa^-}, \qquad [\![\mathbf{q}]\!] = \mathbf{q}^+ \cdot \mathbf{n}_{\kappa^+} + \mathbf{q}^- \cdot \mathbf{n}_{\kappa^-},$$

respectively, where we denote by $\mathbf{n}_{\kappa^\pm}$ the unit outward normal vector of $\partial\kappa^\pm$, respectively. On a boundary edge $F \in \mathcal{F}^{\mathcal{B}}_{\texttt{CFE}}$, we set $\{\!\{v\}\!\} = v$, $\{\!\{\mathbf{q}\}\!\} = \mathbf{q}$, and

$[\![v]\!] = v\mathbf{n}$, with $\mathbf{n}$ denoting the unit outward normal vector on the boundary $\partial\Omega$.

With this notation, we make the following key assumptions, which are the same used in [14]:

(A1) For all elements $\kappa \in \mathcal{T}_{\mathtt{CFE}}$, we define

$$C_\kappa = \operatorname{card}\left\{F \in \mathcal{F}^{\mathcal{I}}_{\mathtt{CFE}} \cup \mathcal{F}^{\mathcal{B}}_{\mathtt{CFE}} : F \subset \partial\kappa\right\}.$$

In the following we assume that there exists a positive constant C_F such that

$$\max_{\kappa\in\mathcal{T}_{\mathtt{CFE}}} C_\kappa \leq C_F,$$

uniformly with respect to the mesh size.

(A2) Inverse inequality. Given an edge $F \in \mathcal{F}^{\mathcal{I}}_{\mathtt{CFE}} \cup \mathcal{F}^{\mathcal{B}}_{\mathtt{CFE}}$ of an element $\kappa \in \mathcal{T}_{\mathtt{CFE}}$, there exists a positive constant C_{inv}, independent of the local mesh size and local polynomial order, such that

$$\|\nabla v\|^2_{L_2(F)} \leq C_{\mathrm{inv}} \frac{p^2}{h_F} \|\nabla v\|^2_{L_2(\kappa)}$$

for all $v \in V(\mathcal{T}_{\mathtt{CFE}}, p)$, where h_F is a *representative* length scale associated to the edge $F \subset \partial\kappa$.

In case that the polynomial degree is not the same on all polygonal elements, also the assumption (A3) as in [14] is needed: We assume that the polynomial degree vector $\boldsymbol{p}$ is of bounded local variation, that is, there is a constant $\rho \geq 1$ such that

$$\rho^{-1} \leq p_\kappa / p_{\kappa'} \leq \rho,$$

whenever κ and κ' share a common edge and p_κ and $p_{\kappa'}$ are their respectively polynomial degrees.

With this notation, we consider the (symmetric) interior penalty hp–DGCFEM for the numerical approximation of (1): find $(\lambda_{j,h}, u_{j,h}) \in \mathbb{R} \times V(\mathcal{T}_{\mathtt{CFE}}, p)$ such that

$$B_{\mathtt{DG}}(u_{j,h}, v) = \lambda_{j,h}(u_{j,h}, v) \tag{2}$$

for all $v \in V(\mathcal{T}_{\mathtt{CFE}}, p)$, where

$$B_{\mathtt{DG}}(u,v) = \sum_{\kappa\in\mathcal{T}_{\mathtt{CFE}}} \int_\kappa \nabla u \cdot \nabla v \, d\mathbf{x} - \sum_{F\in\mathcal{F}^{\mathcal{I}}_{\mathtt{CFE}}\cup\mathcal{F}^{\mathcal{B}}_{\mathtt{CFE}}} \int_F \left(\{\!\{\nabla_h v\}\!\} \cdot [\![u]\!] + \{\!\{\nabla_h u\}\!\} \cdot [\![v]\!] \right) ds$$
$$+ \sum_{F\in\mathcal{F}^{\mathcal{I}}_{\mathtt{CFE}}\cup\mathcal{F}^{\mathcal{B}}_{\mathtt{CFE}}} \int_F \sigma \, [\![u]\!] \cdot [\![v]\!] \, ds,$$
$$(u,v) = \int_\Omega u \, v \, d\mathbf{x}.$$

Here, ∇_h denotes the elementwise gradient operator. Furthermore, the function $\sigma \in L^\infty(\mathcal{F}^{\mathcal{I}}_{\mathtt{CFE}} \cup \mathcal{F}^{\mathcal{B}}_{\mathtt{CFE}})$ is the discontinuity stabilization function that is chosen as follows:

$$\sigma|_F = \gamma p^2 h_F^{-1}, \tag{3}$$

where h_F is the size of the face and with a parameter $\gamma > 0$ that is independent of h_F and p.

We conclude this section by equipping the composite finite element space $V(\mathcal{T}_{\mathtt{CFE}}, p)$ with the DG energy norm $|||\cdot|||_{\mathtt{DG}}$ defined by

$$|||\, v \,|||^2_{\mathtt{DG}} = \sum_{\kappa\in\mathcal{T}_{\mathtt{CFE}}} \|\nabla v\|^2_{L^2(\kappa)} + \sum_{F\in\mathcal{F}^{\mathcal{I}}_{\mathtt{CFE}}\cup\mathcal{F}^{\mathcal{B}}_{\mathtt{CFE}}} \|\sigma^{1/2}[\![v]\!]\|^2_{L^2(F)}.$$

4 A priori analysis

In this section we present a priori results for DGCFEM applied to eigenvalue problems. Throughout the section we assume that Ω is convex so all eigenfunctions of (1) are in $H^s(\Omega)$, with $s \geq 2$.

Lemma 4.1. *Denoting by T and T_h respectively the continuous and the discrete solution operators, for all $f \in L^2(\Omega)$ we have:*

$$|||\,(T - T_h)f\,|||^2_{\mathtt{DG}} \leq C \sum_{\kappa\in\mathcal{T}_{\mathtt{CFE}}} \frac{h_\kappa^{2\min(p+1,s)}}{h_F^2} \frac{1}{p^{2s-3}} \|\mathfrak{E}Tf\|^2_{H^s(\hat{\kappa})}\ , \tag{4}$$

where h_κ is the diameter of the rectangle $\hat{\kappa}$ containing κ, and h_F is the size of the shortest edge of κ.

Proof. By definition, $Tf = u$ and $T_h f = u_h$, then the result is a straightforward application of [14, Theorem 7.2]. □

Remark 4.2. *On meshes of convex well-shape polygons with bounded number of edges, it is admissible to assume that the size of the faces h_F is related to h_κ. In such case* (4) *becomes:*

$$|||\,(T - T_h)f\,|||^2_{\mathtt{DG}} \leq C \sum_{\kappa\in\mathcal{T}_{\mathtt{CFE}}} \frac{h_\kappa^{2\min(p+1,s)-2}}{p^{2s-3}} \|\mathfrak{E}Tf\|^2_{H^s(\hat{\kappa})} \ .$$

The next definition introduces the distance of an approximate eigenfunction from the true eigenspace, which is a crucial quantity in the convergence analysis for eigenvalue problems, especially in the case of non-simple eigenvalues.

Definition 4.3. *Given a function $v \in L^2(\Omega)$ and a finite dimensional subspace $\mathcal{P} \subset L^2(\Omega)$, we define:*

$$\mathrm{dist}(v,\mathcal{P})_{L^2(\Omega)} \ := \ \min_{w\in\mathcal{P}} \|v - w\|_{L^2(\Omega)} \ . \tag{5}$$

Similarly, given a function $v \in S_{\underline{p}}(\mathcal{T})$ and a finite dimensional subspace $\mathcal{P} \subset H^1_0(\Omega)$, we define:

$$\mathrm{dist}(v,\mathcal{P})_{\mathtt{DG}} \ := \ \min_{w\in\mathcal{P}} |||\,v - w\,|||_{\mathtt{DG}} \ . \tag{6}$$

Now let λ_j be any eigenvalue of problem (1) and let $M(\lambda_j)$ denote the span of all corresponding eigenfunctions, moreover let $M_1(\lambda_j) = \{u \in M(\lambda_j) : |||\,u\,|||_{\mathtt{DG}} = 1\}$. Also let us denote for an eigenvalue λ_j of multiplicity R the space $M_h(\lambda_j)$ spanned by all computed eigenfunctions $u_{j+i,h}$, $i = 0,\ldots,R-1$ such that $\lambda_{j+i,h}$ is an approximation of λ_j for all i.

Theorem 4.4. *Suppose that Ω is a convex domain and suppose $1 \leq j \leq \dim V(\mathcal{T}_{\mathtt{CFE}}, p)$. Let λ_j be an eigenvalue of* (1) *with corresponding eigenspace $M(\lambda_j)$ of dimension $R \geq 1$ and let $(\lambda_{j,h}, u_{j,h})$ be an eigenpair of* (2)*. Then, for a sufficiently rich DG finite element space*

(i)

$$|\lambda_j - \lambda_{j,hp}| \ \leq C_1^2 \sum_{\kappa\in\mathcal{T}_{\mathtt{CFE}}} \frac{h_\kappa^{2\min(p+1,s)}}{h_F^2} \frac{1}{p^{2s-3}} \ , \tag{7}$$

(ii)

$$\mathrm{dist}(u_{j,hp}, M_1(\lambda_j))_{E,\mathcal{T}} \ \leq \ C_1 \sum_{\kappa\in\mathcal{T}_{\mathtt{CFE}}} \frac{h_\kappa^{\min(p+1,s)}}{h_F} \frac{1}{p^{s-3/2}} \ , \tag{8}$$

where $h := \max_{\kappa \in \mathcal{T}_{\mathtt{CFE}}} h_\kappa$ *and the constant* C_1 *is independent of* h *and* p.

Proof. In order to prove (i) we recall equation (3.18) from [17], *i.e.*,

$$|\lambda_j - \lambda_{j,hp}| \;\leq\; \sup_{0 \leq i \leq R} |\lambda_j - \lambda_{j+i,hp}| \;\leq\; C \sup_{\substack{u \in M(\lambda_j) \\ |||\, u \,|||_{\mathtt{DG}}=1}} \inf_{v_h \in V(\mathcal{T}_{\mathtt{CFE}},p)} |||\, u - v_h \,|||^2_{\mathtt{DG}} \;.$$

Then the result comes from [14, Theorem 7.2].

In order to prove (ii) we use the arguments in [18]. In particular we have that if λ_j is an eigenvalue of (1), then it is straightforward to see that $\mu_j = \lambda_j^{-1}$ is an eigenvalue of T. Let Γ be a circle in the complex plane centered at μ_j which does not enclose any other point of $\sigma(T)$. As in [18, Sections 5-6], using the spectral projections

$$E = \frac{1}{2\pi i} \int_\Gamma (z - T)^{-1}\, dz \;, \quad E_h = \frac{1}{2\pi i} \int_\Gamma (z - T_h)^{-1}\, dz \;,$$

we have

$$\begin{aligned} \operatorname{dist}(u_{j,hp}, M_1(\lambda_j))_{\mathtt{DG}} \;&\leq\; \sup_{\substack{u_h \in M_h(\lambda_j) \\ |||\, u_h \,|||_{\mathtt{DG}}=1}} \inf_{v \in M_1(\lambda_j)} |||\, v - u_h \,|||_{\mathtt{DG}} \\ &=\; \sup_{\substack{u_h \in V(\mathcal{T}_{\mathtt{CFE}},p) \\ |||\, u_h \,|||_{\mathtt{DG}}=1}} \inf_{v \in L^2(\Omega)} |||\, Ev - E_h u_h \,|||_{\mathtt{DG}} \;. \end{aligned}$$

Then taking $v = u_h$ we have

$$\begin{aligned} \operatorname{dist}(u_{j,hp}, M_1(\lambda_j))_{\mathtt{DG}} \;&\leq\; \sup_{\substack{u_h \in V(\mathcal{T}_{\mathtt{CFE}},p) \\ |||\, u_h \,|||_{\mathtt{DG}}=1}} |||\, Eu_h - E_h u_h \,|||_{\mathtt{DG}} \\ &=\; \|E - E_h\|_{\mathcal{L}(V(\mathcal{T}_{\mathtt{CFE}},p),V(\mathcal{T}_{\mathtt{CFE}},p))} \;\leq\; \|E - E_h\|_{\mathcal{L}(L^2(\Omega),V(\mathcal{T}_{\mathtt{CFE}},p))} \;. \end{aligned}$$

Using an argument similar to [17, Theorem 3.11], we have that

$$\|E - E_h\|_{\mathcal{L}(L^2(\Omega),V(\mathcal{T}_{\mathtt{CFE}},p))} \;\leq\; C\|T - T_h\|_{\mathcal{L}(L^2(\Omega),V(\mathcal{T}_{\mathtt{CFE}},p))} \;.$$

To conclude the proof we use (4).

□

5 Numerical experiments

In this section we present a series of computational examples to numerically investigate the asymptotic convergence behaviour of the proposed DGCFEM for eigenvalue problems on polygonal meshes. Throughout this section the DGCFEM eigenpairs (λ_h, u_h) defined by (2) are computed with the constant γ, appearing in the interior penalty parameter σ defined by (3), equal to 10. All the numerical examples presented in this section have been computed using the AptoFEM package (`www.aptofem.com`) and solving the resulting generalised eigenvalue problem with ARPACK [19] and the Multifrontal Massively Parallel Solver (MUMPS), see [20, 21, 22].

5.1 Example 1: Meshes of polygons

In this first example, we consider a sequence of seven polygonal meshes for the unit square. The meshes are generated using `PolyMesher` [23] with a high number of smoothing iterations in order to obtain meshes formed by quite regular polygons. The meshes contain respectively 25, 50, 100, 200, 400, 800 and 1600 polygons, see Figure 1 for two examples of polygonal meshes.

In order to show that the approximation properties of such meshes are comparable to standard meshes of triangles or rectangles, we present the approximation error for the first three distinct eigenvalues on the sequence of meshes and using different order of polynomials.

From Figures 2, 3 and 4, we observe that the rates of convergence of the error $|\lambda - \lambda_h|$ on the sequence of polygonal meshes for $p = 1, 2, 3$ is optimal for the first three distinct eigenvalues. The multiplicity 2 of the second eigenvalue does not seem to affect the convergence rates.

In Figure 5 we present the convergence for the first three distinct eigenvalues increasing the order of p uniformly and using the mesh number 4 in the sequence. The convergence rates seem close to exponential in both the value of p and the number of degrees of freedom. This is in agreement with the theory.

5.2 Example 2: Meshes of non-regular polygons

In this second example, we investigate the effect of the regularity of the polygons forming the meshes on the approximation error for eigenvalues for the same problem has in the first example. This time the sequence of seven

meshes is generated using `PolyMesher` [23] with a very low number of smoothing iterations in order to obtain meshes formed by non-regular polygons. The meshes contain respectively 25, 50, 100, 200, 400, 800 and 1600 polygons, see Figure 6 for two examples of polygonal meshes.

From Figures 7, 8 and 9, we observe that the rate of convergence of the error $|\lambda - \lambda_h|$ on the sequence of polygonal meshes for $p = 1, 2, 3$ is optimal for the first three distinct eigenvalues. The convergence rates seem only very moderately affected by the non-regularity of the polygons.

In Figure 10 we present the convergence for the first three distinct eigenvalues increasing the order of p uniformly and using the mesh number 4 in the sequence. Also in this case, the convergence rates seem only very moderately affected by the non-regularity of the polygons.

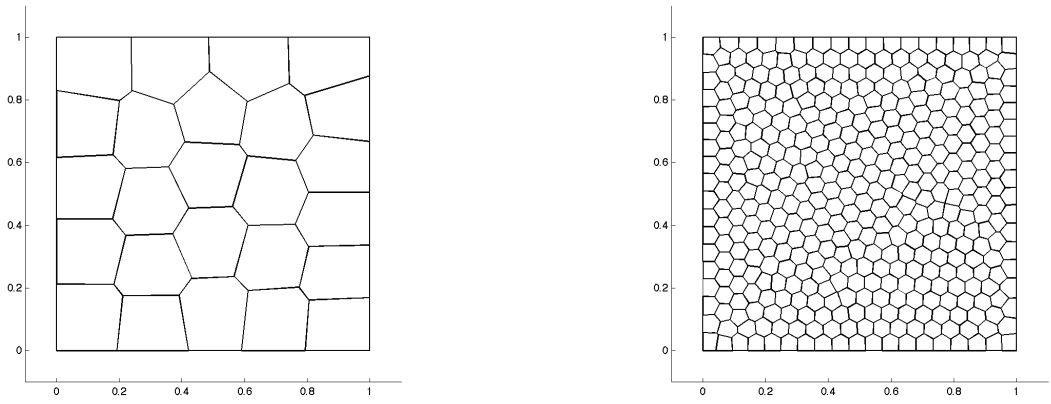

(a) (b)

Figure 1: Example 1: (a) Polygonal mesh number 1 containing 25 polygons. (b) Polygonal mesh number 5 containing 400 polygons.

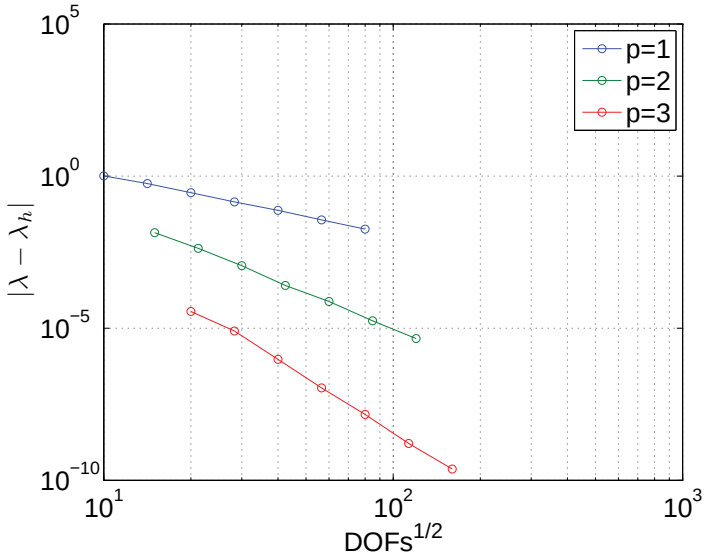

Figure 2: Example 1: Convergence of the approximated first eigenvalue on the sequence of polygonal meshes using polynomials of order 1, 2 and 3.

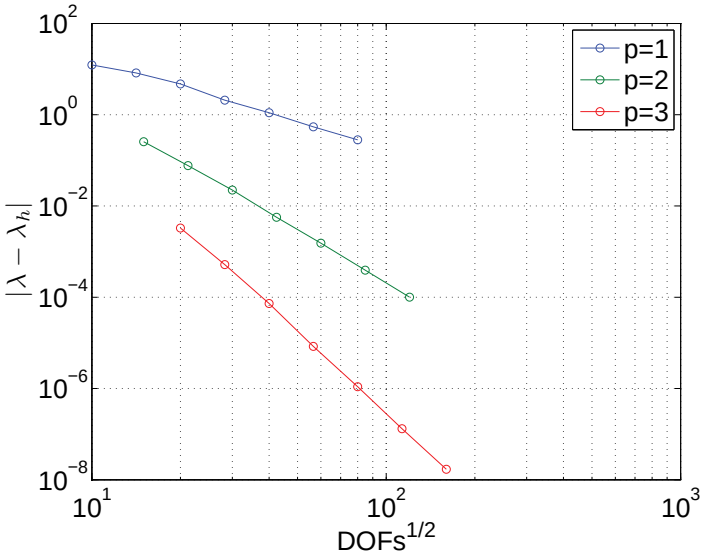

Figure 3: Example 1: Convergence of the approximated second eigenvalue on the sequence of polygonal meshes using polynomials of order 1, 2 and 3.

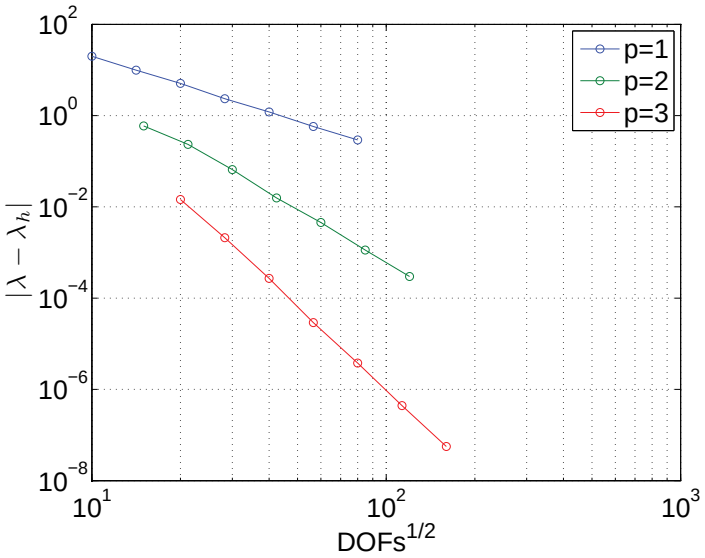

Figure 4: Example 1: Convergence of the approximated third eigenvalue on the sequence of polygonal meshes using polynomials of order 1, 2 and 3.

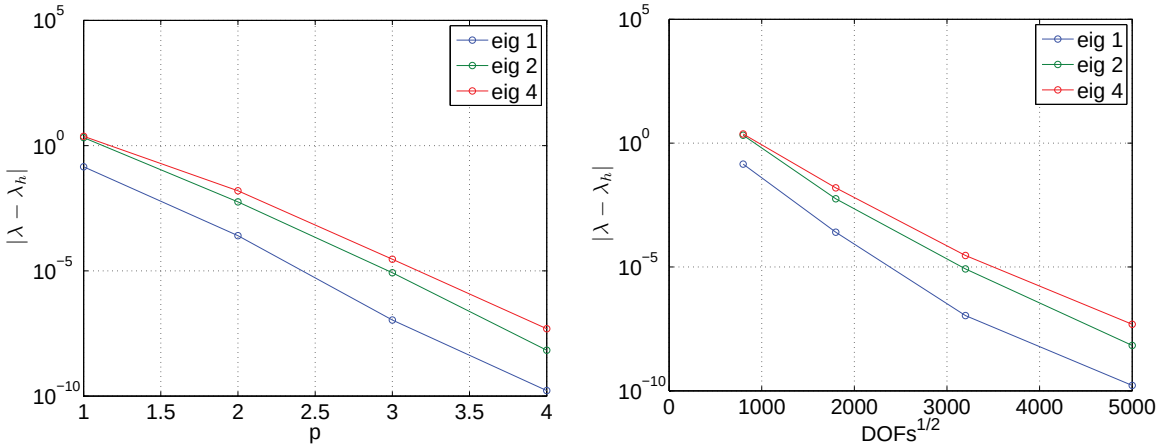

(a) (b)

Figure 5: Example 1: (a) Convergence of the first three distinct eigenvalues in the order of p and (b) in the numbers of DOFs for uniform refinement in p.

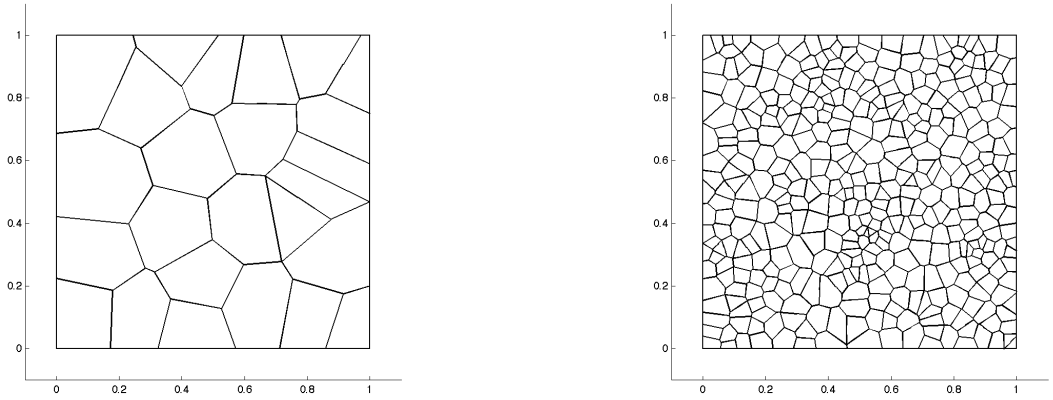

(a) (b)

Figure 6: Example 2: (a) Polygonal mesh number 1 containing 25 polygons. (b) Polygonal mesh number 5 containing 400 polygons.

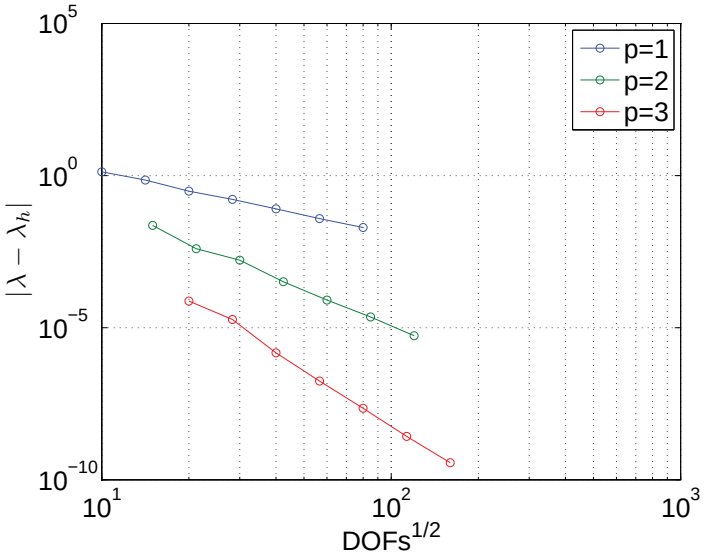

Figure 7: Example 2: Convergence of the approximated first eigenvalue on the sequence of polygonal meshes using polynomials of order 1, 2 and 3.

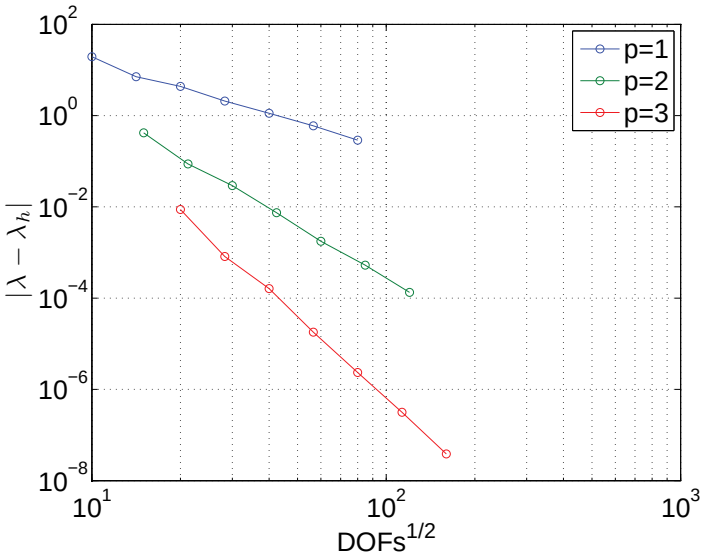

Figure 8: Example 2: Convergence of the approximated second eigenvalue on the sequence of polygonal meshes using polynomials of order 1, 2 and 3.

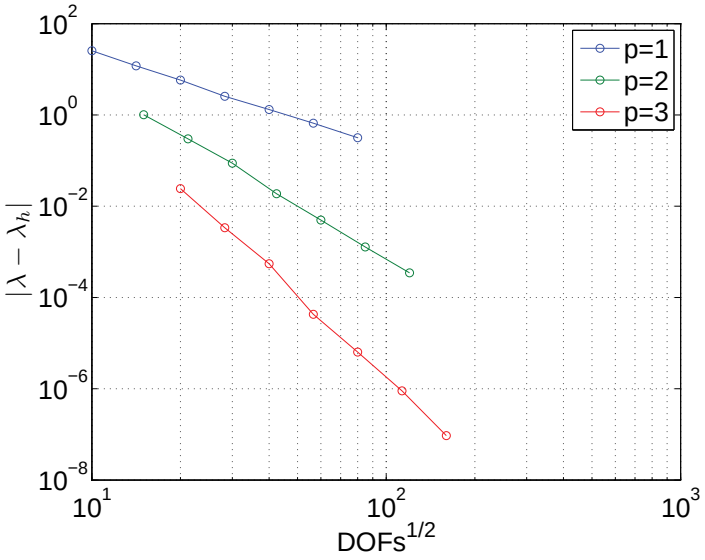

Figure 9: Example 2: Convergence of the approximated third eigenvalue on the sequence of polygonal meshes using polynomials of order 1, 2 and 3.

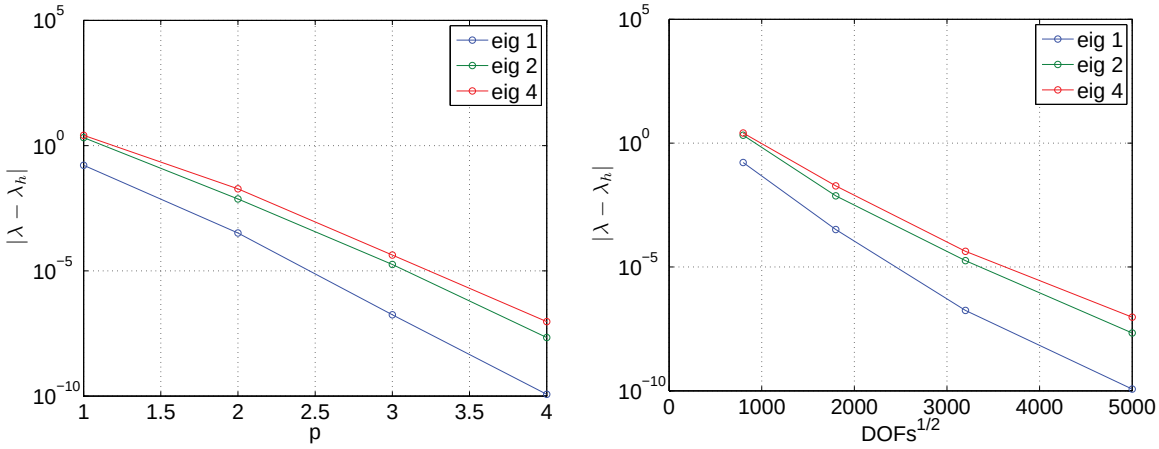

(a) (b)

Figure 10: Example 2: (a) Convergence of the first three distinct eigenvalues in the order of p and (b) in the numbers of DOFs for uniform refinement in p.

5.3 Example 3: Non-convex polygons

In this third example, we investigate the approximation properties of non-convex polygons. In order to do that we use a pathological configuration where there are elements completely surrounded by single elements, see Figure 11. This kind of configuration is common for certain applications like in photonic crystals [24, 25, 26].

In Figures 12 and 13 we present the convergence for the first three distinct eigenvalues increasing the order of p uniformly and using the meshes in Figure 11. It is very interesting to notice that good convergence rates are obtained also for these pathological meshes.

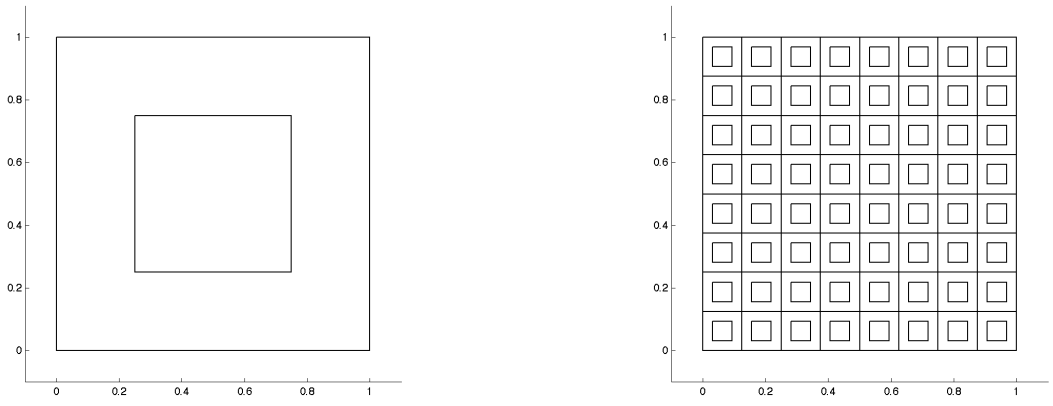

(a) (b)

Figure 11: Example 3: (a) A mesh formed by two elements one completely surrounding the other. (b) A mesh constructed by repeating the configuration in (a).

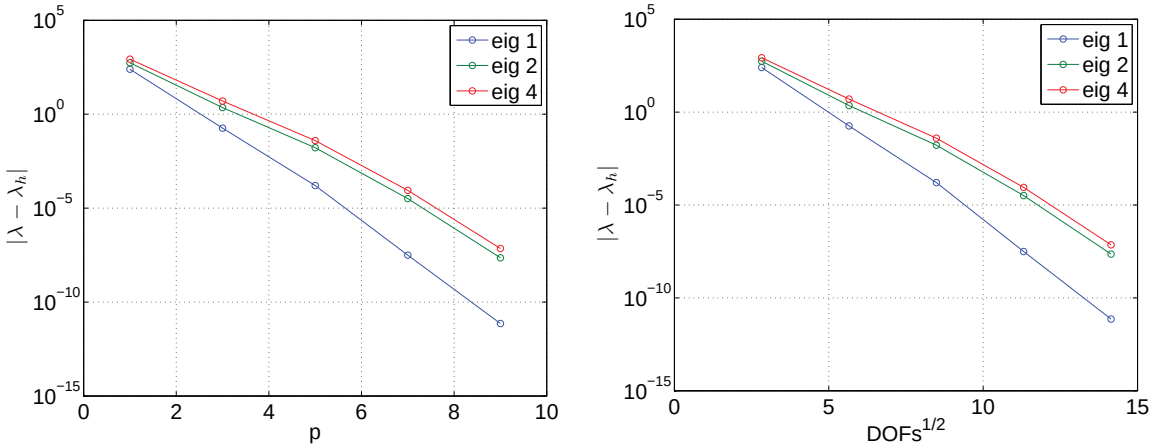

(a) (b)

Figure 12: Example 1: (a) Convergence of the first three distinct eigenvalues in the order of p and (b) in the numbers of DOFs for uniform refinement in p for the mesh in Figure 11(a).

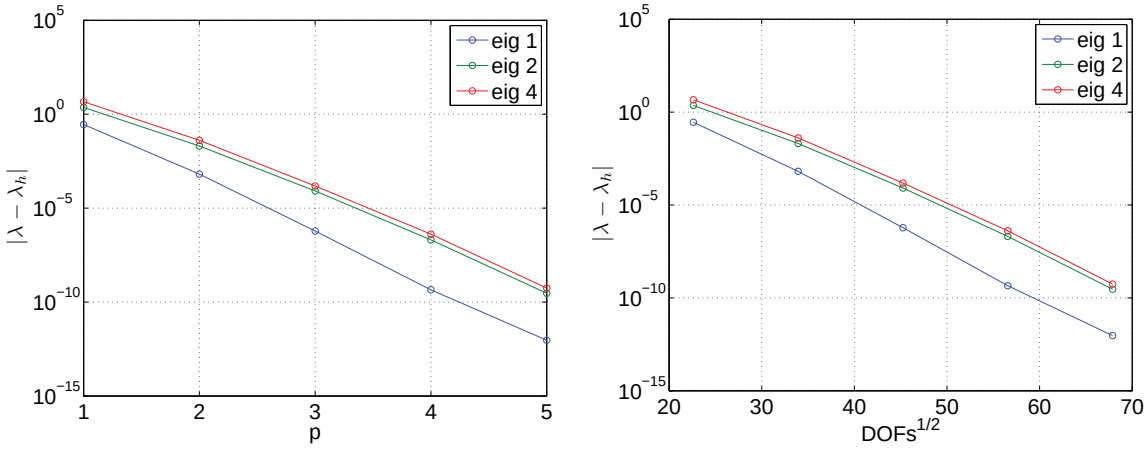

Figure 13: Example 1: (a) Convergence of the first three distinct eigenvalues in the order of p and (b) in the numbers of DOFs for uniform refinement in p for the mesh in Figure 11(b).

5.4 Example 4: Discontinuous potential

In this fourth example, we explore a more complicated problem:

$$\begin{cases} -\Delta u + \mathcal{B} u &= \lambda\, u \qquad \text{in } \Omega, \\ \\ u &= 0 \qquad \text{on } \partial\Omega. \end{cases}$$

where $\mathcal{B}$ is piecewise constant. We consider a sequence of polygonal meshes of the unit square where $\mathcal{B}$ can assume two different values. The meshes are generated using `PolyMesher` with an high number of smoothing iterations in order to obtain meshes formed by quite regular polygons. The meshes contain respectively 24, 50, 100, 200, 400, 800 and 1600 polygons, see Figure 14 for two examples of polygonal meshes. In the blue region $\mathcal{B} = 100$ and in the yellow region $\mathcal{B} = 1$. The eigenfunctions of such problem are contained in $H^2(\Omega)$ and so the theory presented so far can be applied to this case as well.

In order to study that the approximation properties for such problem, we present the approximation error for the first four eigenvalues on the sequence of meshes and using different order of polynomials. From Figures 15, 16, 17 and 18, we observe that the rates of convergence of the error $|\lambda - \lambda_h|$ on the sequence of polygonal meshes for $p = 1, 2, 3$ are asymptotically optimal for the first four eigenvalues.

In Figure 19 we present the convergence for the first four distinct eigenvalues increasing the order of p uniformly and using the mesh number 4 in the sequence. The convergence rates seem close to exponential in both the value of p and the number of degrees of freedom. This is in agreement with the theory since the jump in the potential term do not affect the global regularity of the eigenfunctions.

In order to check that the same could be achievable for problems where the interface between the two regions is more complicated, we took the mesh number 5 from the first example Figure 1(b) and we set $\mathcal{B} = 1$ in all polygonal elements with the center within the circle of radius 0.25 and centred in (0.5,0.5) and $\mathcal{B} = 100$ otherwise. The convergence rates for the first four eigenvalues for uniform refinement in p are presented in Figure 20. Also in this case the convergence curves approximate exponential functions even if the convergence rates are not settled yet.

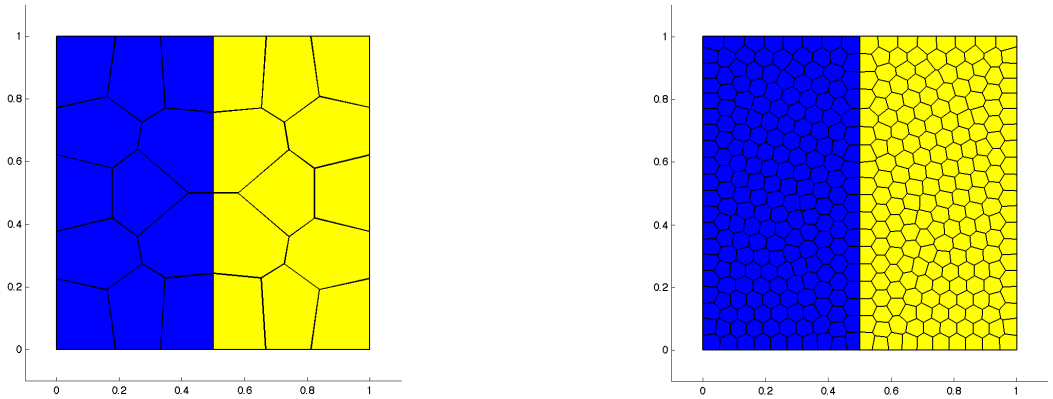

(a) (b)

Figure 14: Example 4: (a) Polygonal mesh number 1 containing 24 polygons. (b) Polygonal mesh number 5 containing 400 polygons. The two colours denote the two regions where $\mathcal{B}$ assumes different values.

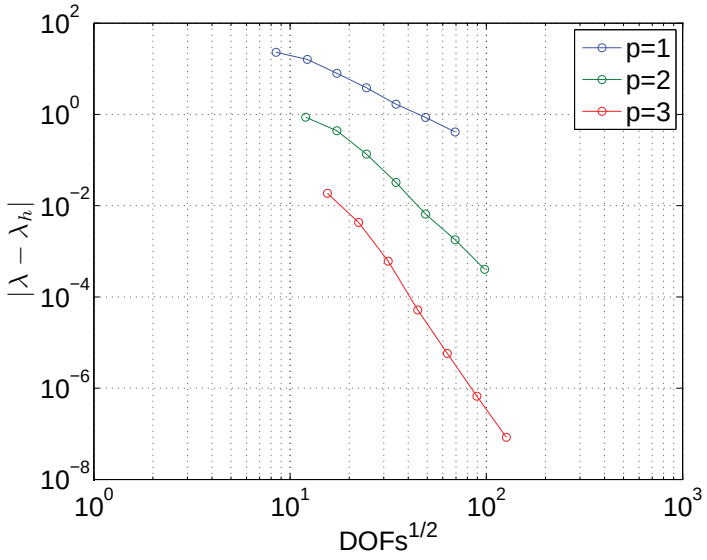

Figure 15: Example 4: Convergence of the approximated first eigenvalue on the sequence of polygonal meshes using polynomials of order 1, 2 and 3.

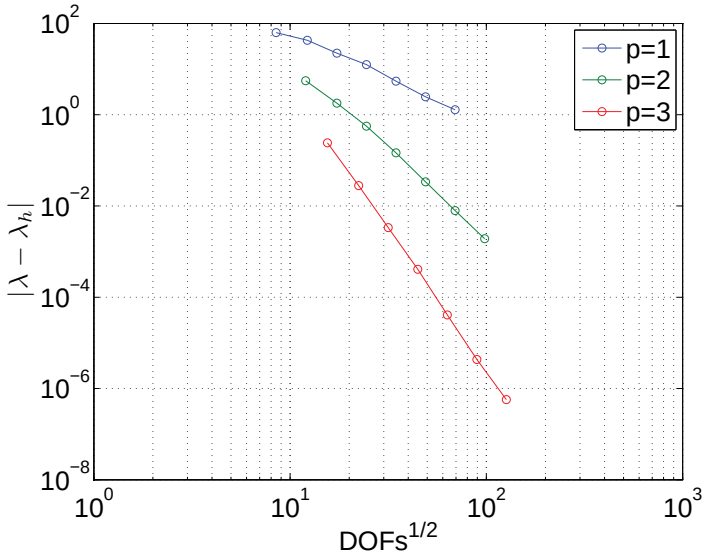

Figure 16: Example 4: Convergence of the approximated second eigenvalue on the sequence of polygonal meshes using polynomials of order 1, 2 and 3.

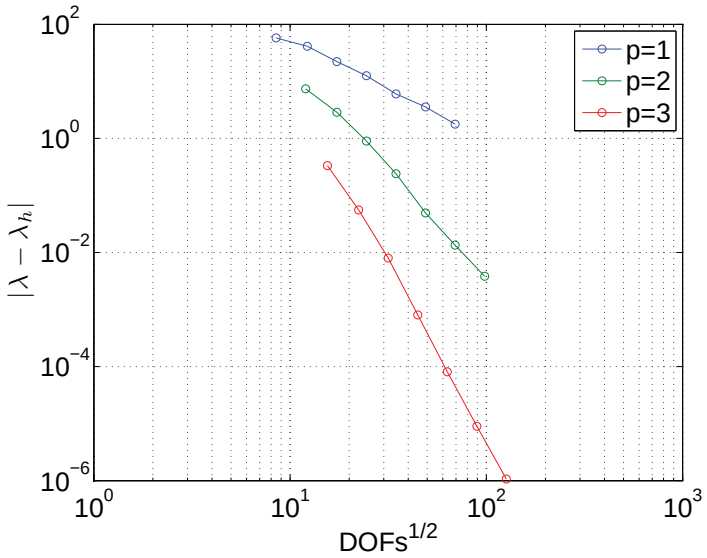

Figure 17: Example 4: Convergence of the approximated third eigenvalue on the sequence of polygonal meshes using polynomials of order 1, 2 and 3.

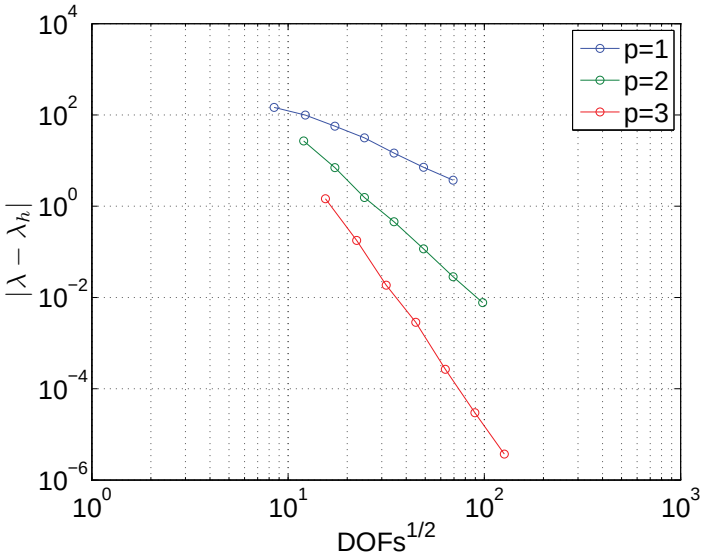

Figure 18: Example 4: Convergence of the approximated fourth eigenvalue on the sequence of polygonal meshes using polynomials of order 1, 2 and 3.

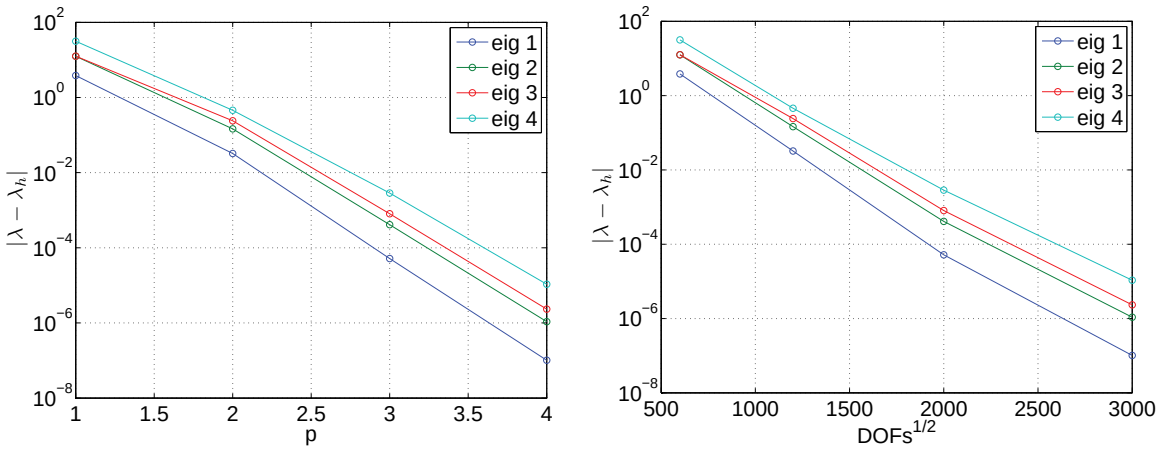

(a) (b)

Figure 19: Example 4: (a) Convergence of the first three distinct eigenvalues in the order of p and (b) in the numbers of DOFs for uniform refinement in p.

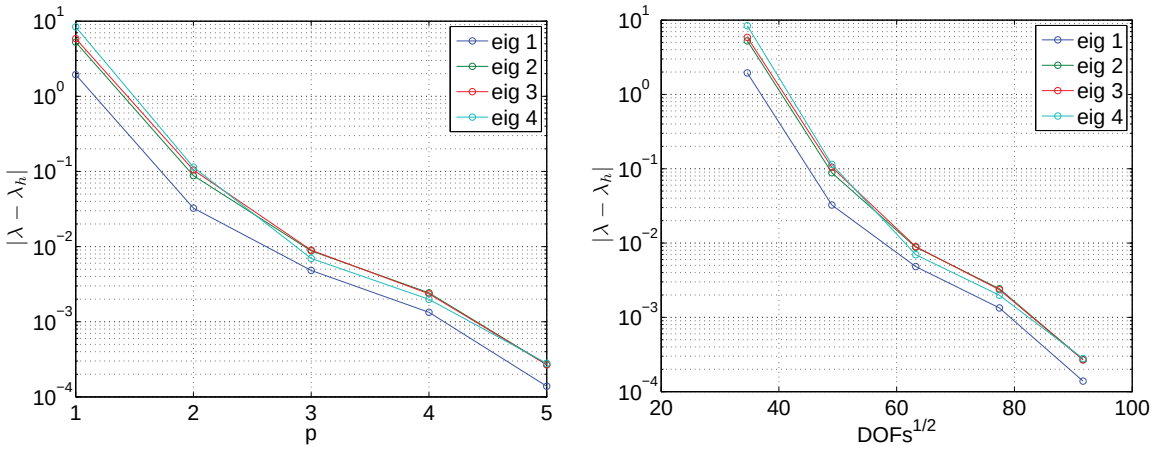

Figure 20: Example 4: (a) Convergence of the first three distinct eigenvalues in the order of p and (b) in the numbers of DOFs for uniform refinement in p.

5.5 Example 5: Discontinuous second order term

In this last example, we study the behaviour of polygonal meshes for problems with discontinuous coefficients in the second order term: In this fourth example, we explore a more complicated problem:

$$\begin{cases} -\nabla \cdot (\mathcal{A}\nabla u) &= \lambda\, u \qquad \text{in } \Omega, \\ \\ u &= 0 \qquad \text{on } \partial\Omega. \end{cases}$$

where $\mathcal{A}$ is piecewise constant. The sequence of meshes used in this example are the same as in the previous example, see Figure 14. This problem has been chosen because standard finite element elements achieve exponential convergence rate for such configuration when p is increased. This is due to the fact that, even if a discontinuous coefficient in the second order term can in general lead to lack of regularity in the eigenfunctions, for this particular case where the interface between regions with different values of $\mathcal{A}$ is smooth, the eigenfunctions are still in $H^2(\Omega)$. Our aim is to check that also for polygonal meshes the same behaviour is achieved. In particular we set $\mathcal{A} = 1$ in the yellow region and $\mathcal{A} = 10$ in the blue region.

From Figures 21, 22, 23 and 24, we observe that the rates of convergence of the error $|\lambda - \lambda_h|$ on the sequence of polygonal meshes for $p = 1, 2, 3$ are asymptotically optimal for the first four eigenvalues.

In Figure 25 we present the convergence for the first three distinct eigenvalues increasing the order of p uniformly and using the mesh number 4 in the sequence. The convergence rates seem close to exponential in both the value of p and the number of degrees of freedom.

6 Concluding remarks

In this article we have considered the extension of the discontinuous Galerkin composite finite element technique to polygonal meshes for eigenvalue problems. This extension is very attractive as meshes of polygons arise naturally in many applications due to the geometries involved in such problems.

In this article we have undertaken the a priori error analysis for DGCFEM for eigenvalue problems on polygonal meshes and we have illustrate the convergence in practise with a series of numerical examples. For sake of completeness we have considered examples with discontinuous coefficient as well.

Overall the convergence rates for polygonal meshes are comparable to the convergence rates for standard meshes, even when the polygons are not very regular.

References

[1] W. Hackbusch, S. Sauter, Composite finite elements for the approximation of PDEs on domains with complicated micro-structures, Numer. Math. 75 (1997) 447–472.

[2] W. Hackbusch, S. Sauter, Composite finite elements for problems containing small geometric details. Part II: Implementation and numerical results, Comput. Visual Sci. 1 (1997) 15–25.

[3] M. Rech, S. Sauter, A. Smolianski, Two-scale composite finite element method for the dirichlet problem on complicated domains, Numer. Math. 102 (4) (2006) 681–708.

[4] W. Hackbusch, S. A. Sauter, Composite finite elements for problems containing small geometric details (Jul. 1997). doi:10.1007/s007910050002.
URL http://link.springer.com/article/10.1007/s007910050002

[5] W. Hackbusch, S. A. Sauter, Composite finite elements for the approximation of PDEs on domains with complicated micro-structures (Feb. 1997). doi:10.1007/s002110050248.
URL http://link.springer.com/article/10.1007/s002110050248

[6] N. Sukumar, A. Tabarraei, Conforming polygonal finite elements, International Journal for Numerical Methods in Engineering 61 (12) (2004) 2045–2066. doi:10.1002/nme.1141.
URL http://onlinelibrary.wiley.com/doi/10.1002/nme.1141/abstract

[7] A. Tabarraei, N. Sukumar, Extended finite element method on polygonal and quadtree meshes, Computer Methods in Applied Mechanics and Engineering 197 (5) (2008) 425–438. doi:10.1016/j.cma.2007.08.013.
URL http://www.sciencedirect.com/science/article/pii/S0045782507003374

[8] T.-P. Fries, T. Belytschko, The extended/generalized finite element method: An overview of the method and its applications, International

Journal for Numerical Methods in Engineering 84 (3) (2010) 253–304. doi:10.1002/nme.2914.
URL http://onlinelibrary.wiley.com/doi/10.1002/nme.2914/abstract

[9] L. BEIRO DA VEIGA, F. BREZZI, A. CANGIANI, G. MANZINI, L. D. MARINI, A. RUSSO, BASIC PRINCIPLES OF VIRTUAL ELEMENT METHODS, Mathematical Models and Methods in Applied Sciences 23 (01) (2012) 199–214. doi:10.1142/S0218202512500492.
URL http://www.worldscientific.com/doi/abs/10.1142/S0218202512500492

[10] A. Cangiani, E. H. Georgoulis, P. Houston, hp-version discontinuous galerkin methods on polygonal and polyhedral meshes, Mathematical Models and Methods in Applied Sciences 24 (10) (2014) 2009–2041. doi:10.1142/S0218202514500146.
URL http://www.worldscientific.com/doi/abs/10.1142/S0218202514500146

[11] F. Bassi, L. Botti, A. Colombo, D. A. Di Pietro, P. Tesini, On the flexibility of agglomeration based physical space discontinuous galerkin discretizations, Journal of Computational Physics 231 (1) (2012) 45–65. doi:10.1016/j.jcp.2011.08.018.
URL http://www.sciencedirect.com/science/article/pii/S0021999111005055

[12] F. Bassi, L. Botti, A. Colombo, S. Rebay, Agglomeration based discontinuous galerkin discretization of the euler and navierstokes equations, Computers & Fluids 61 (2012) 77–85. doi:10.1016/j.compfluid.2011.11.002.
URL http://www.sciencedirect.com/science/article/pii/S0045793011003367

[13] F. Bassi, L. Botti, A. Colombo, Agglomeration-based physical frame dG discretizations: An attempt to be mesh free, Mathematical Models and Methods in Applied Sciences 24 (08) (2014) 1495–1539. doi:10.1142/S0218202514400028.
URL http://www.worldscientific.com/doi/abs/10.1142/S0218202514400028

[14] P. Antonietti, S. Giani, P. Houston, *hp*–Version composite discontinuous Galerkin methods for elliptic problems on complicated domains, SIAM J. Sci. Comput. 35 (3) (2013) A1417–A1439.

[15] S. Giani, P. Houston, hp-adaptive composite discontinuous galerkin methods for elliptic problems on complicated domains, Numerical Methods for Partial Differential Equations (accepted).

[16] S. Giani, P. Houston, Goal-oriented adaptive composite discontinuous galerkin methods for incompressible flows, Journal of Computational and Applied Mathematics 270 (2014) 32–42. doi:10.1016/j.cam.2014.03.007.
URL http://www.sciencedirect.com/science/article/pii/S0377042714001472

[17] P. Antonietti, Domain decomposition, spectral correctness and numerical testing of discontinuous galerkin methods, Ph.D. thesis, (2006).

[18] P. Antonietti, A. Buffa, I. Perugia, Discontinuous galerkin approximation of the laplace eigenproblem, J. Comput. Appl. Math. 204 (2) (2007) 317–333.

[19] R. B. Lehoucq, D. C. Sorensen, C. Yang, ARPACK users' guide, Vol. 6 of Software, Environments, and Tools, Society for Industrial and Applied Mathematics (SIAM), Philadelphia, PA, 1998, solution of large-scale eigenvalue problems with implicitly restarted Arnoldi methods.

[20] P. R. Amestoy, I. S. Duff, J. Koster, J.-Y. L'Excellent, A fully asynchronous multifrontal solver using distributed dynamic scheduling, SIAM Journal on Matrix Analysis and Applications 23 (1) (2001) 15–41.

[21] P. R. Amestoy, I. S. Duff, J.-Y. L'Excellent, Multifrontal parallel distributed symmetricand unsymmetric solvers, Comput. Methods Appl. Mech. Eng. 184 (2000) 501–520.

[22] P. R. Amestoy, A. Guermouche, J.-Y. L'Excellent, S. Pralet, Hybrid scheduling for the parallel solution of linear systems, Parallel Computing 32 (2) (2006) 136–156.

[23] C. Talischi, G. H. Paulino, A. Pereira, I. F. M. Menezes, PolyMesher: a general-purpose mesh generator for polygonal elements written in matlab, Structural and Multidisciplinary Optimization 45 (3) (2012) 309–328. doi:10.1007/s00158-011-0706-z.
URL http://link.springer.com/article/10.1007/s00158-011-0706-z

[24] S. Giani, An a posteriori error estimator for hp-adaptive continuous galerkin methods for photonic crystal applications, Computing 95 (5) (2013) 395–414.

[25] S. Giani, I. Graham, Adaptive finite element methods for computing band gaps in photonic crystals, Numerische Mathematik 121 (1) (2012) 31–64.

[26] S. Giani, An a posteriori error estimator for hp-adaptive discontinuous galerkin methods for computing band gaps in photonic crystals, Journal of Computational and Applied Mathematics 236 (18) (2012) 4810–4826.

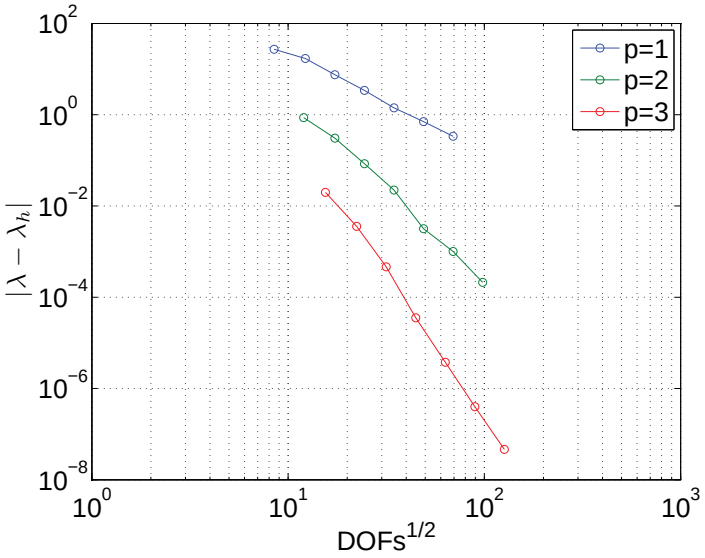

Figure 21: Example 5: Convergence of the approximated first eigenvalue on the sequence of polygonal meshes using polynomials of order 1, 2 and 3.

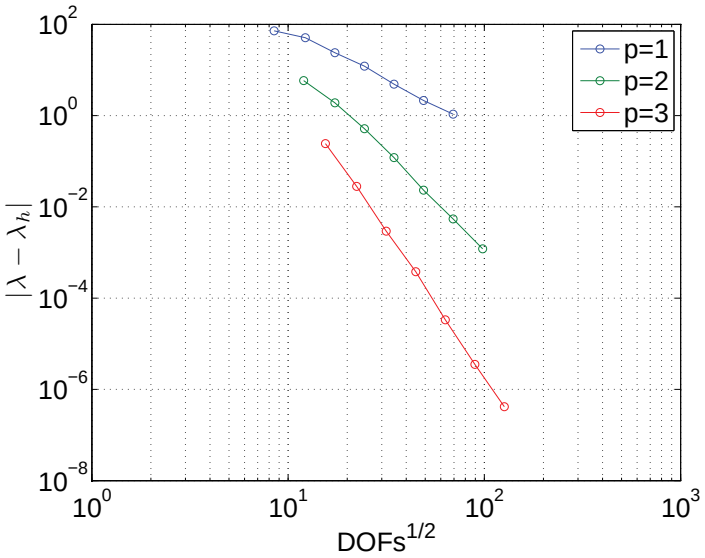

Figure 22: Example 5: Convergence of the approximated second eigenvalue on the sequence of polygonal meshes using polynomials of order 1, 2 and 3.

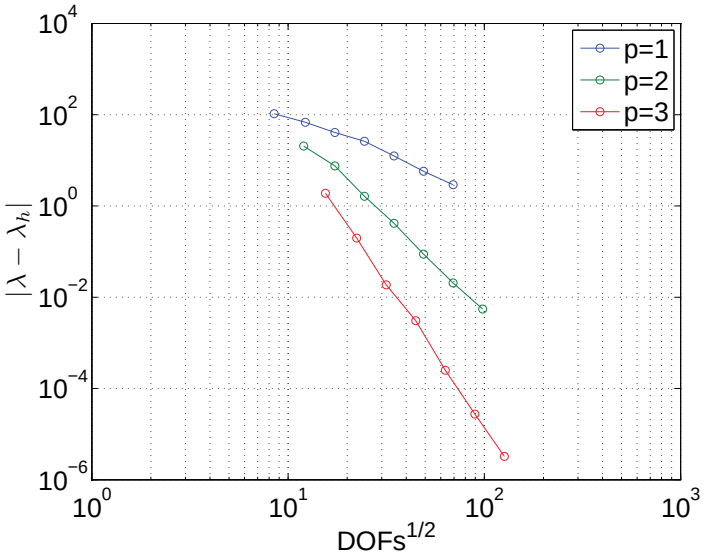

Figure 23: Example 5: Convergence of the approximated third eigenvalue on the sequence of polygonal meshes using polynomials of order 1, 2 and 3.

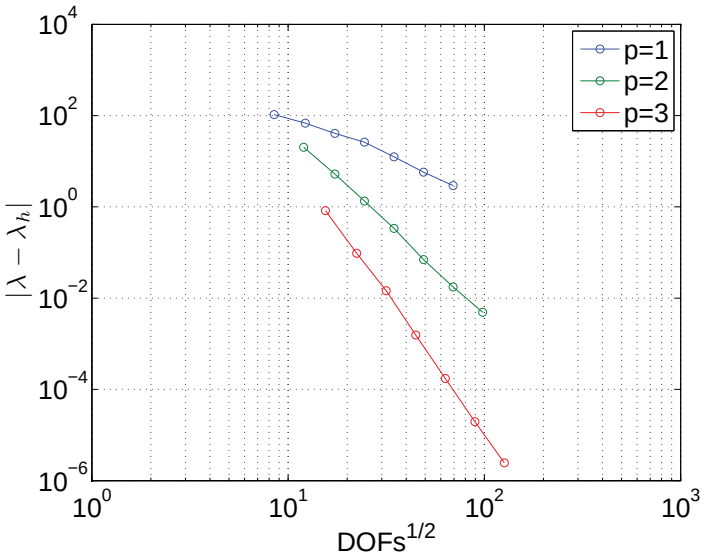

Figure 24: Example 5: Convergence of the approximated fourth eigenvalue on the sequence of polygonal meshes using polynomials of order 1, 2 and 3.

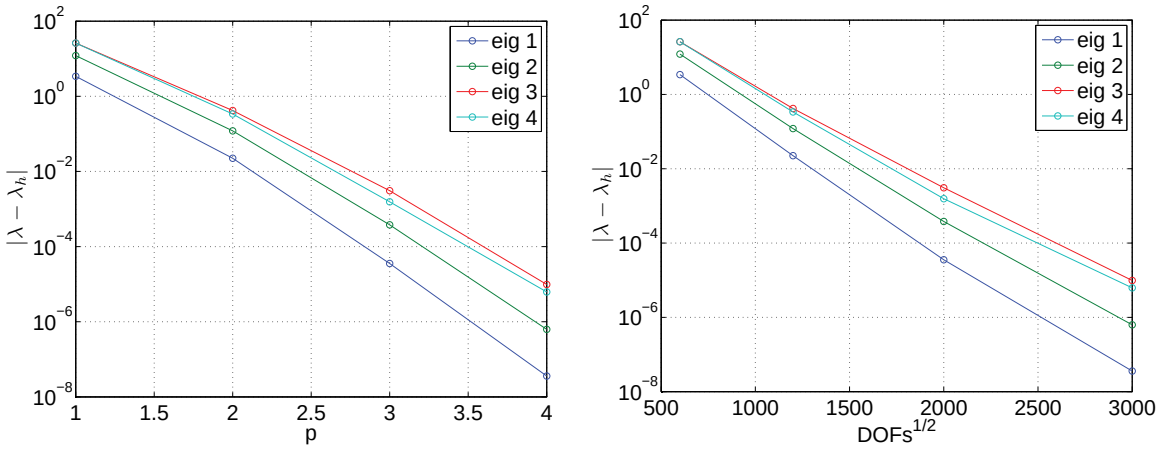

Figure 25: Example 5: (a) Convergence of the first three distinct eigenvalues in the order of p and (b) in the numbers of DOFs for uniform refinement in p.